Geomechanics and Engineering, *Vol. 19, No. 2 (2019) 141-151*
DOI: https://doi.org/10.12989/gae.2019.19.2.141

Created cavity expansion solution in anisotropic and drained condition based on Cam-Clay model

Chao Li* and Jin-Feng Zou[a]

School of Civil Engineering, Central South University, Hunan 410075, China

(Received February 13, 2019, Revised September 12, 2019, Accepted September 26, 2019)

Abstract. A novel theoretical solution is presented for created (zero initial radius) cavity expansion problem based on Cam-Clay model and considers the effect of initial anisotropic in-situ stress and drained conditions. Here the strain of this theoretical solution is small deformation in elastic region and large deformation in plastic region. The works for cylindrical and spherical cavities expanding in drained condition from zero initial radius are investigated. Most of the conventional solutions were based on the isotropic and undrained condition, however, the initial stress state of natural soil mass is anisotropy by soil deposition history, and drained cavity expansion calculation is closer to actual engineering in permeable soil mass. Finally, the parametric study is presented in order to the engineering significance of this work.

Keywords: theoretical solution; created cavity expansion problem; cam-clay model; initial anisotropic in-situ stress; drained condition; large deformation

1. Introduction

Over the last seven decades, a large amount of papers has been published for cavity expansion problem in geomechanic and geotechnical engineering. Cavity expansion method (CEM) can be used to piling, in-situ testing, grouting and tunneling, and so on. A large amount of model can be used to investigate the cavity expansion problem for different rock and soil materials, and consider the loading condition, hardening/softening condition and drained condition. Some CEM can be written as follows: theoretical research (Hill *et al.* 1944, Bishop *et al.* 1945, Vesic 1977, Teh and Houlsby 1991, Yu and Carter 2002, Randolph 2003, Park *et al.* 2008, Tolooiyan and Gavin 2011, Chen and Abousleiman 2012, Wang *et al.* 2012a, b, Pournaghiazar *et al.* 2013, Lukic *et al.* 2014, Zhou *et al.* 2014, Zou *et al.* 2017, Zhou *et al.* 2018, Sivasithamparam and Castro 2018, Li *et al.* 2019a, b); engineering applications (Frikha and Bouassida 2014, Frikha *et al.* 2015, Keawsawasvong and Ukritchon 2016, Kwon *et al.* 2018, Chen *et al.* 2019, Zou *et al.* 2019a, b); numerical simulations and experiments (Salgado and Randolph 2001, Seo *et al.* 2012, Marchi *et al.* 2014, Diao *et al.* 2014, Xiao and Desai 2016); and others.

Nevertheless, a large amount of papers for cavity expansion problem basically focus on isotropic geomaterials, undrained condition and finite sized initial cavity problem in both region (elastic and plastic regions).

Less research has been carried out on the created cavity expansion problem based on Cam-Clay model and considers the effect of initial anisotropic in-situ stress and drained conditions. The initial stress state of soil mass is anisotropy by soil deposition history (Anderson 1980, Zhou *et al.* 2014). The solutions of the created cavity expansion problem based on Cam-Clay model were produced for cylindrical cavities which model the action of the pressuremeter, and for spherical cavities that may be used to estimate cone tip resistance and bearing capacity of displacement piles (Collins and Yu 1996). In addition, the works for cylindrical and spherical cavities expanding in drainage condition from zero initial radius are investigated. Most of the conventional solutions were based on the undrained condition for the low permeable soils. However, the drained cavity expansion calculation is presented in order to the study of cavity expansion problem in permeable soil mass. Only very recently, a few papers presented theoretical analysis investigating initial anisotropic in-situ stress and drained conditions in saturated soil mass. Hill (1950) and Yu and Carter (2002) presented the incremental velocity solutions to analyze CEM in the Tresca soil mass for the created cavity expansion problem. Zhou *et al.* (2014) presented the elastic-plastic theoretical solutions to analyze CEM in the Tresca soil mass under anisotropic initial stress and undrained condition. Then, some works were presented for investigate the effect of stress anisotropy in undrained condition (Li *et al.* 2016, Sivasithamparam and Castro 2018). Russell and Khalili (2002) presented the similarity solutions to analyze CEM in the Mohr-Coulomb soil mass for the drained cavity expansion problem.

Comparing with other elasto-plastic models, the Cam-Clay model (Roscoe *et al.* 1958, 1963) is one of the most widely used models in the field of soil mechanics at present. Its main characteristics are: the clear basic concept, better suited for normal consolidated and weak over-consolidated

*Corresponding author, Ph.D. Student
E-mail: lichao@csu.edu.cn
[a]Professor
E-mail: zoujinfeng_csu@163.com

ISSN: 2005-307X (Print), 2092-6219 (Online)

soil mass, as well as only three parameters (it can be obtained by conventional triaxial test), which is easy to popularization in geotechnical engineering practice. The yield characteristics of hydrostatic pressure, shear shrinkage and compressive hardening of geotechnical materials are considered. At present, although the ideas of various model for geomaterials are emerging, and various forms of soil constitutive models have emerged, but the Cam-Clay model is one of the few recognized elasto-plastic models. The Cam-Clay elasto-plastic constitutive model is regarded as the beginning of modern soil mechanics and also is one of the most widely used models in the field of soil mechanics. The critical state theory developed by based on this model has more explicit geometric and physical meanings, which is unmatched by many other elasto-plastic models. In addition, the improvement and correction of its limitations based on the Cam-Clay model is still an important direction for geotechnical material model, which needs further study (Li 2004).

In a word, a large amount of papers for cavity expansion problem basically focus on isotropic geomaterials, undrained condition and finite sized initial cavity problem. Less research has been carried out on the created cavity expansion problem based on Cam-Clay model and considers the effect of initial anisotropic in-situ stress and drained conditions. The main objective of this study is to develop a theoretical solution, on the basis of Cam-Clay model and initial anisotropic in-situ stress. Eventually, the parametric study is presented in order to the engineering significance of this work.

2. Theory and methodology

2.1 Problem definition and assumptions

2.1.1 Problem definition

Fig. 1 shows a quasi-static cavity expansion in soil mass subjected to an initial in-situ horizontal stress σ_{h0} (i.e., the hydrostatic stress), an initial vertical stress σ_{v0}, as well as an initial pore water pressure u_0, the initial anisotropic stress factor (k_0) represents the ratio of the effective horizontal stress to the effective vertical stress. The cavity expands from zero initial radius to the current radius a when the increase of the internal pressure from 0 to p, the cavity first experience elastic deformation and then plastic deformation when the inner cavity is loaded. A plastic region around the cavity will then be formed from the current radius a to the elastic-plastic boundary r_b, as well as the intermediate state is shown as in Fig. 1. The radial displacement of r_b is u_{rb}.

2.1.2 Assumptions

Some assumptions can be written:

(1) The Cam-Clay model was originally proposed by Roscoe *et al.* (1958), it has a simple unified mathematical expression (Roscoe *et al.* 1963, Schofield and Wroth, 1968). For soil mass around the cavity, the yield failure criterion based on the Cam-Clay model can be expressed,

$$q = Mp' \tag{1}$$

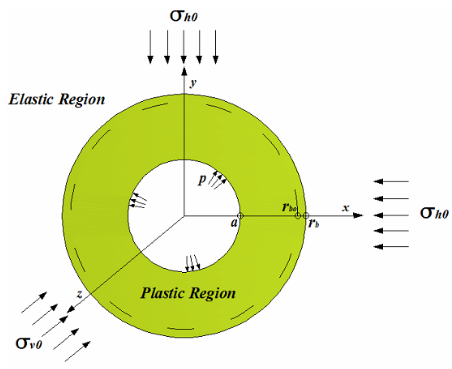

Fig. 1 The intermediate state for created cavity expansion problem

where, the magnitude of M for cylindrical cavity can be determined using M=6sinφ/(3-sinφ), the magnitude of M for spherical cavity can be determined using M=2sinφ, and φ is the internal friction angle.

The p' is the mean effective stress, and the q is the deviator stress, respectively, as follows (Collins and Yu 1996),

$$p' = \frac{\sigma_r' + k\sigma_\theta'}{1+k} \tag{2}$$

$$q = \sigma_r' - \sigma_\theta' = \sigma_r - \sigma_\theta \tag{3}$$

where, k is a variable representing the type of cavity (k=1, spherical cavity; k=2, cylindrical cavity). σ_r and σ_θ are the radial and tangential stresses, σ'_r and σ'_θ are the effective radial and tangential stresses, respectively.

Combining Eqs. (1), (2) and (3),

$$\sigma_r' = \frac{1+k+Mk}{1+k-M}\sigma_\theta' \tag{4}$$

(2) In the small-strain theory, the radial strain can be determined using $\varepsilon_r = -\partial(du)/\partial r$, the tangential strain can be determined using $\varepsilon_\theta = u/r$.

(3) In the large-strain theory, the radial natural strain can be determined using $d\varepsilon_r = du/r$, the tangential natural strain can be determined using $d\varepsilon_\theta = -du/r$.

(4) Based on the stress-strain theory of Yu and Carter (2002), the stress-strain relation in elastic region is expressed in differential form by Young's modulus E, Poisson's ratio v and the type variable of cavity k.

$$\left.\begin{aligned} d\varepsilon_r^e &= \frac{1-v^2(2-k)}{E}\left(d\sigma_r - \frac{kv}{1-v(2-k)}d\sigma_\theta\right) \\ d\varepsilon_\theta^e &= \frac{1-v^2(2-k)}{E}\left((1-v(k-1))d\sigma_\theta - \frac{v}{1-v(2-k)}d\sigma_r\right) \\ M' &= \frac{E}{1-v^2(2-k)} \end{aligned}\right\} \tag{5}$$

2.2 Elastic region

In both region, the equilibrium equation can be expressed,

$$\frac{d\sigma_r}{dr}+k\frac{\sigma_r-\sigma_\theta}{r}=0 \tag{6}$$

The boundary condition are expressed as, $\sigma_r(r=\infty)=\sigma_{h0}$, $\sigma_r(r=r_b)=\sigma_{rb}$.

The stresses and displacement around the cavity in elastic region,

$$\begin{cases}\sigma_r=\sigma_{h0}+\left(\sigma_{rb}-\sigma_{h0}\right)\left(\dfrac{r_b}{r}\right)^{k+1}\\ \sigma_\theta=\sigma_{h0}-\dfrac{\left(\sigma_{rb}-\sigma_{h0}\right)}{k}\left(\dfrac{r_b}{r}\right)^{k+1}\end{cases} \tag{7}$$

$$u=\frac{\left(\sigma_{rb}-\sigma_{h0}\right)r_b}{2kG}\left(\frac{r_b}{r}\right)^{k} \tag{8}$$

The displacement around the cavity at the position of r_b,

$$u_{rb}=\frac{\left(\sigma_{rb}-\sigma_{h0}\right)r_b}{2kG} \tag{9}$$

2.3 EP boundary analysis

Based on the paper of Yu and Carter (2002), the plastic radius (r_b) in drained condition is investigated. For drained case, the pore water pressure remains constant and thus can be subtracted out of the analysis (Chen and Abousleiman 2017).

According to Eq. (4) and the aforementioned drained condition,

$$\begin{cases}d\sigma_r=Rd\sigma_\theta\\ R=\dfrac{1+k+Mk}{1+k-M}\end{cases} \tag{10}$$

In plastic region, the non-associated flow law can be expressed,

$$\begin{cases}d\varepsilon_{rp}^{p}/d\varepsilon_{\theta p}^{p}=\left(d\varepsilon_{rp}-d\varepsilon_{rp}^{e}\right)/\left(d\varepsilon_{\theta p}-d\varepsilon_{\theta p}^{e}\right)=-k/\beta\\ \beta=\left(1+\sin\psi\right)/\left(1-\sin\psi\right)\end{cases} \tag{11}$$

where ψ is the dilation angle. ε_{rp} and $\varepsilon_{\theta p}$ the radial and tangential strains in plastic region. ε^{p}_{rp} and $\varepsilon^{p}_{\theta p}$ are the radial and tangential plastic strains in plastic region. ε^{e}_{rp} and $\varepsilon^{e}_{\theta p}$ are the radial and tangential elastic strains in plastic region.

Combining Eqs. (5) and (11),

$$\begin{aligned}\beta d\varepsilon_r+d\varepsilon_\theta=&\frac{\left(1-\nu^2(2-k)\right)\left(\beta-\left(k\nu/(1-\nu(2-k))\right)\right)}{E}d\sigma_r\\ &+\frac{\left(1-\nu^2(2-k)\right)\left(k(1-2\nu)+2\nu-(k\beta\nu)/(1-\nu(2-k))\right)}{E}d\sigma_\theta\\ =&\frac{1}{M}\left[\beta-\left(k\nu/(1-\nu(2-k))\right)\right]d\sigma_r\\ &+\frac{1}{M}\left[k(1-2\nu)+2\nu-(k\beta\nu)/(1-\nu(2-k))\right]d\sigma_\theta\end{aligned} \tag{12}$$

Combining the Eq. (10), $d\sigma_\theta=(1/R)d\sigma_r$ can be obtained, the yield Eq. (12) can be derived,

$$\begin{cases}d\varepsilon_r+\left(k/\beta\right)d\varepsilon_\theta=\left(\xi/\beta\right)d\sigma_r\\ \xi=\dfrac{1}{M'}\left[\begin{array}{l}\left(\beta-\left(k\nu/(1-\nu(2-k))\right)\right)\\ +\dfrac{1+k-M}{M'(1+k+Mk)}\left(\begin{array}{l}k(1-2\nu)+2\nu\\ -(k\beta\nu)/(1-\nu(2-k))\end{array}\right)\end{array}\right]\end{cases} \tag{13}$$

Based on Yu's definition, the continuous deformation around the cavity is geometrically self-similar. The symbol V is defined as the relative velocity. A little incrementation of the plastic radius is dr_b, the corresponding displacement of a particle around the cavity is du, $du=dr=Vdr_b$, u is a function of the current radius r and r_b. Namely, r_b and r are two independent variables. The total differential of u is expressed,

$$\begin{aligned}du&=\left(\partial u/\partial r_b\right)dr_b+\left(\partial u/\partial r\right)dr\\ &=\left(\partial u/\partial r_b\right)dr_b+V\left(\partial u/\partial r\right)dr_b\end{aligned} \tag{14}$$

The particle velocity,

$$V=\left(\partial u/\partial r_b\right)/\left(1-\partial u/\partial r\right) \tag{15}$$

For a given particle around the cavity,

$$\begin{cases}d\varepsilon_r=-\partial\left(du\right)/\partial r=-\left(\partial V/\partial r\right)dr_b\\ d\varepsilon_\theta=-du/r=-\left(Vdr_b\right)/r\\ d\sigma_r=\left(\left(\partial\sigma_r/\partial r_b\right)+V\left(\partial\sigma_r/\partial r\right)\right)dr_b\\ d\sigma_\theta=\left(\left(\partial\sigma_\theta/\partial r_b\right)+V\left(\partial\sigma_\theta/\partial r\right)\right)dr_b\end{cases} \tag{16}$$

So, the Eq. (13) can also be expressed,

$$\frac{kV}{\beta r}+\frac{\partial V}{\partial r}=-\left(\xi/\beta\right)\left(V\frac{\partial\sigma_r}{\partial r}+\frac{\partial\sigma_r}{\partial r_b}\right) \tag{17}$$

Therefore,

$$\begin{cases}P(r)V+\dfrac{\partial V}{\partial r}=Q(r)\\ P(r)=\dfrac{k}{\beta r}-\dfrac{\xi\sigma_{rb}k(Mk+M)}{\left(1+k+Mk\right)\beta r}\left(\dfrac{r_b}{r}\right)^{k\frac{Mk+M}{1+k+Mk}}\\ Q(r)=-\dfrac{s}{r_b}\left(\dfrac{r_b}{r}\right)^{k\frac{Mk+M}{1+k+Mk}}\\ s=\dfrac{\xi\sigma_{rb}k\left(Mk+M\right)}{\left(1+k+Mk\right)\beta}\end{cases} \tag{18}$$

According to Eq. (8),

$$V_{r=r_b}=\frac{\left(\sigma_{rb}-\sigma_{h0}\right)}{2kG}(1+k) \tag{19}$$

The Eq. (18) can also be written,

$$V=\exp\left[-\frac{\xi\sigma_{rb}}{\beta}\left(\frac{r_b}{r}\right)^{k\frac{Mk+M}{1+k+Mk}}\right]\left\{\begin{array}{l}\sum_{n=0}^{\infty}H_n\left(\frac{r_b}{r}\right)^{\frac{k(Mk+M)(1+n)}{1+k+Mk}-1}\\ +\left[\begin{array}{l}\frac{\left(\sigma_{rb}-\sigma_{h0}\right)}{2kG}(k+1)\exp\left(\frac{\xi\sigma_{rb}}{\beta}\right)\\ -\sum_{n=0}^{\infty}H_n\end{array}\right]\left(\frac{r_b}{r}\right)^{\frac{k}{\beta}}\end{array}\right\} \tag{20}$$

where,

$$H_n=\frac{1}{n!}\left(\frac{\xi\sigma_{rb}}{\beta}\right)^n\frac{\beta s}{\left[k+\beta-k\beta(\frac{Mk+M}{1+k+Mk})(1+n)\right]} \tag{21}$$

According to V=da/dr$_b$ at the cavity wall (r=a),

$$\frac{da}{dr_b}=\exp\left[-\frac{\xi\sigma_{rb}}{\beta}\left(\frac{r_b}{r}\right)^{k\frac{Mk+M}{1+k+Mk}}\right]\left\{\begin{array}{l}\sum_{n=0}^{\infty}H_n\left(\frac{r_b}{r}\right)^{\frac{k(Mk+M)(1+n)}{1+k+Mk}-1}\\ +\left[\begin{array}{l}\frac{\left(\sigma_{rb}-\sigma_{h0}\right)}{2kG}(k+1)\exp\left(\frac{\xi\sigma_{rb}}{\beta}\right)\\ -\sum_{n=0}^{\infty}H_n\end{array}\right]\left(\frac{r_b}{r}\right)^{\frac{k}{\beta}}\end{array}\right\} \tag{22}$$

The geometrically self-similar around the cavity can be expressed,

$$\frac{da}{dr_b}=\frac{a}{r_b} \tag{23}$$

The ratio of the radius of cavity (a) to the plastic radius (r$_b$) can be written,

$$\frac{a}{r_b}=\exp\left[-\frac{\xi\sigma_{rb}}{\beta}\left(\frac{r_b}{r}\right)^{k\frac{Mk+M}{1+k+Mk}}\right]\left\{\begin{array}{l}\sum_{n=0}^{\infty}H_n\left(\frac{r_b}{r}\right)^{\frac{k(Mk+M)(1+n)}{1+k+Mk}-1}\\ +\left[\begin{array}{l}\frac{\left(\sigma_{rb}-\sigma_{h0}\right)}{2kG}(k+1)\exp\left(\frac{\xi\sigma_{rb}}{\beta}\right)\\ -\sum_{n=0}^{\infty}H_n\end{array}\right]\left(\frac{r_b}{r}\right)^{\frac{k}{\beta}}\end{array}\right\} \tag{24}$$

The plastic radius r$_b$ can be easily derived if the radius of cavity a is determined.

2.4 Plastic region

2.4.1 The total stresses

Combining Eqs. (7) and (10),

$$\begin{cases}\sigma_{rp}=\frac{(k+1)\sigma_{h0}\left(1+k+M\right)}{(k+1)^2}\\ \sigma_{\theta p}=\frac{(k+1)\sigma_{h0}\left(1+k-M\right)}{(k+1)^2}\end{cases} \tag{25}$$

Combining Eqs. (6) and (10),

$$\sigma_r=K\left(\frac{1}{r}\right)^{k\frac{Mk+M}{1+k+Mk}} \tag{26}$$

Combining Eqs. (25), (26) and the boundary conditions,

$$K=\left(\frac{(k+1)\sigma_{h0}\left(1+k+Mk\right)}{(k+1)^2}\right)r_b^{k\frac{Mk+M}{1+k+Mk}} \tag{27}$$

Combining Eqs. (26) and (27), the total radial stress is derived,

$$\sigma_r=\left(\frac{(k+1)\sigma_{h0}\left(1+k+Mk\right)}{(k+1)^2}\right)\left(\frac{r_b}{r}\right)^{k\frac{Mk+M}{1+k+Mk}} \tag{28}$$

Combining Eq. (28) and (10), the tangential stress is derived,

$$\sigma_\theta=\frac{1}{R}\left[\left(\frac{(k+1)\sigma_{h0}\left(1+k+Mk\right)}{(k+1)^2}\right)\left(\frac{r_b}{r}\right)^{k\frac{Mk+M}{1+k+Mk}}\right] \tag{29}$$

2.4.1 Limit expanded pressure

According to the Eq. (28), the limit expanded pressure is expressed,

$$\sigma_r\left(r=a_u\right)=p_u \tag{30}$$

$$p_u=\sigma_{rb}\left(\frac{r_b}{a_u}\right)^{k\frac{Mk+M}{1+k+Mk}} \tag{31}$$

3. Validation and discussions

To confirm the validity of this solution, the calculation parameters are selected (Yu and Carter 2002), σ_{h0}=100 kPa, the Poisson's ratio v=0.3, G/p$_0$=10, 100 and 1000, $\varphi=20^0\sim50^0$, $\psi=0^0\sim\varphi$, u$_0$=0. As shown in Table 1 and Table 2, the presented results is very close to Yu's theoretical results, which confirms the validity of this presented solution.

To analyze the effect of the initial anisotropic in-situ stress by introducing the initial anisotropic stress factor (k$_0$) into the theoretical solution in drained cavity expansion condition, the calculation parameters are selected (Yu and Carter, 2002), σ_{h0}=100kPa(k$_0$=1), the Poisson's ratio v=0.3, E=2600, $\varphi=20^0\sim50^0$, $\psi=0^0\sim\varphi$.

As shown in Tables 3-6, the effect of initial anisotropic stress factor k$_0$ on the radius ratio (r$_b$/a) and the normalized internal pressure (p/σ_{h0}) are investigated. It is noted that the effect of the initial value of k$_0$ on the r$_b$/a of cavity expansion problem is investigated, and five cases with the same other parameters but different values of k$_0$ are studied,

Table 1 The results (r_b/a) of this presented solution and Yu and Carter (2002)

φ^0	ψ^0	$2G_0/\sigma_{h0}$	r_b/a, k=1, (Yu and Carter 2002)	rb/a, k=1, the presented solution	Error (%)	r_b/a, k=2, (Yu and Carter, 2002)	rb/a, k=2, the presented solution	Error (%)
20	0	20	4.74	4.7411	0.02%	2.63	2.6316	0.06%
		200	14.57	14.5712	0.01%	5.49	5.494	0.07%
		2000	45.77	45.7762	0.01%	11.74	11.7362	-0.03%
	10	20	6.06	6.0621	0.03%	3.23	3.2321	0.07%
		200	22.46	22.4629	0.01%	7.97	7.9701	0.00%
		2000	85.86	85.8644	0.01%	20.39	20.3898	0.00%
	20	20	7.64	7.6379	-0.03%	3.99	3.9872	-0.07%
		200	33.82	33.8176	-0.01%	11.68	11.6759	-0.04%
		2000	156.10	156.1276	0.02%	36.15	36.1476	-0.01%
30	0	20	3.98	3.9783	-0.04%	2.32	2.3153	-0.20%
		200	12.11	12.1129	0.02%	4.78	4.7834	0.07%
		2000	37.92	37.9156	-0.01%	10.16	10.1637	0.04%
	10	20	4.90	4.9022	0.04%	2.73	2.7344	0.16%
		200	17.85	17.854	0.02%	6.58	6.5797	0.00%
		2000	67.76	67.7577	0.00%	16.59	16.5916	0.01%
	20	20	5.95	5.9489	-0.02%	3.22	3.2237	0.11%
		200	25.62	25.6202	0.00%	9.00	9.0034	0.04%
		2000	116.80	116.7952	0.00%	26.96	26.9619	0.01%
	30	20	7.08	7.0766	-0.05%	3.77	3.7669	-0.08%
		200	35.45	35.4497	0.00%	12.05	12.0497	0.00%
		2000	191.00	191.1786	0.09%	42.25	42.2522	0.01%
40	0	20	3.55	3.5502	0.01%	2.12	2.1215	0.07%
		200	10.74	10.7365	-0.03%	4.35	4.3529	0.07%
		2000	33.50	33.4974	-0.01%	9.20	9.2038	0.04%
	10	20	4.27	4.2713	0.03%	2.44	2.4422	0.09%
		200	15.34	15.3395	0.00%	5.76	5.7624	0.04%
		2000	57.79	57.7945	0.01%	14.31	14.3133	0.02%
	20	20	5.06	5.0597	-0.01%	2.80	2.7977	-0.08%
		200	21.28	21.2828	0.01%	7.51	7.5141	0.05%
		2000	95.67	95.7303	0.06%	21.72	21.7211	0.01%
	30	20	5.88	5.8801	0.00%	3.17	3.1719	0.06%
		200	28.44	28.444	0.01%	9.51	9.514	0.04%
		2000	150.03	150.0607	0.02%	31.21	31.2058	-0.01%
	40	20	6.69	6.6881	-0.03%	3.54	3.5428	0.08%
		200	36.42	36.4292	0.03%	11.59	11.5902	0.00%
		2000	220.42	220.3937	-0.01%	41.69	41.6925	0.01%
50	0	20	3.28	3.2819	0.06%	1.99	1.9904	0.02%
		200	9.88	9.8788	-0.01%	4.07	4.0672	-0.07%
		2000	30.74	30.7374	-0.01%	8.57	8.566	-0.05%
	10	20	3.89	3.8851	-0.13%	2.25	2.2516	0.07%
		200	13.80	13.8024	0.02%	5.24	5.2357	-0.08%
		2000	51.66	51.6641	0.01%	12.83	12.8291	-0.01%
	20	20	4.53	4.5284	-0.04%	2.53	2.5313	0.05%
		200	18.69	18.693	0.02%	6.60	6.5995	-0.01%

Table 1 Continued

φ^0	ψ^0	$2G_0/\sigma_{h0}$	r_b/a, k=1, (Yu and Carter, 2002)	rb/a, k=1, the presented solution	Error (%)	r_b/a, k=2, (Yu and Carter, 2002)	rb/a, k=2, the presented solution	Error (%)
50	20	2000	83.02	83.0343	0.02%	18.49	18.4886	-0.01%
	30	20	5.18	5.1818	0.03%	2.82	2.8156	-0.16%
		200	24.37	24.3716	0.01%	8.05	8.0536	0.04%
		2000	125.93	125.9393	0.01%	25.00	25.0001	0.00%
	40	20	5.81	5.8112	0.02%	3.09	3.0884	-0.05%
		200	30.47	30.4757	0.02%	9.47	9.4684	-0.02%
		2000	178.64	178.8595	0.12%	31.48	31.4822	0.01%
	50	20	6.38	6.3819	0.03%	3.33	3.3344	0.13%
		200	36.51	36.508	-0.01%	10.73	10.7315	0.01%
		2000	237.19	237.0757	-0.05%	37.21	37.2075	-0.01%

Table 2 The results (p/σ_{h0}) of this presented solution and Yu and Carter (2002)

φ^0	ψ^0	$2G_0/\sigma_{h0}$	r_b/a, k=1, (Yu and Carter, 2002)	rb/a, k=1, the presented solution	Error (%)	r_b/a, k=2, (Yu and Carter, 2002)	rb/a, k=2, the presented solution	Error (%)
20	0	20	2.97	2.9665	-0.12%	4.06	4.0614	0.03%
		200	5.26	5.2575	-0.05%	8.60	8.601	0.01%
		2000	9.42	9.4225	0.03%	18.65	18.6458	-0.02%
	10	20	3.36	3.3624	0.07%	5.01	5.0082	-0.04%
		200	6.55	6.5552	0.08%	12.57	12.5677	-0.02%
		2000	12.98	12.9838	0.03%	32.74	32.7426	0.01%
	20	20	3.78	3.7827	0.07%	6.20	6.2034	0.05%
		200	8.08	8.075	-0.06%	18.55	18.548	-0.01%
		2000	17.61	17.6097	0.00%	58.70	58.6948	-0.01%
30	0	20	3.77	3.766	-0.11%	5.51	5.513	0.05%
		200	7.91	7.9111	0.01%	14.51	14.5067	-0.02%
		2000	16.93	16.9282	-0.01%	39.63	39.6253	-0.01%
	10	20	4.33	4.3285	-0.03%	6.88	6.8824	0.03%
		200	10.25	10.2461	-0.04%	22.19	22.1912	0.01%
		2000	24.93	24.9288	0.00%	76.16	76.164	0.01%
	20	20	4.92	4.9246	0.09%	8.57	8.5714	0.02%
		200	13.04	13.0354	-0.04%	33.71	33.7116	0.00%
		2000	35.84	35.8379	-0.01%	145.51	145.5106	0.00%
	30	20	5.53	5.5287	-0.02%	10.55	10.5495	0.00%
		200	16.18	16.1861	0.04%	49.72	49.7207	0.00%
		2000	49.74	49.7755	0.07%	264.82	264.8632	0.02%
40	0	20	4.43	4.4276	-0.05%	6.78	6.7845	0.07%
		200	10.53	10.5263	-0.04%	20.90	20.8951	-0.02%
		2000	25.64	25.6431	0.01%	67.45	67.4523	0.00%
	10	20	5.12	5.117	-0.06%	8.46	8.4567	-0.04%
		200	13.92	13.9165	-0.03%	32.41	32.4125	0.01%
		2000	39.29	39.295	0.01%	134.62	134.6293	0.01%
	20	20	5.84	5.8424	0.04%	10.46	10.4615	0.01%
		200	17.98	17.9814	0.01%	49.10	49.1057	0.01%
		2000	58.30	58.3234	0.04%	258.59	258.6089	0.01%

Table 2 Continued

φ^0	ψ^0	$2G_0/\sigma_{h0}$	r_b/a, k=1, (Yu and Carter, 2002)	rb/a, k=1, the presented solution	Error (%)	r_b/a, k=2, (Yu and Carter 2002)	rb/a, k=2, the presented solution	Error (%)
40	30	20	6.57	6.5714	0.02%	12.73	12.7324	0.02%
		200	22.56	22.5629	0.01%	71.04	71.0443	0.01%
		2000	82.90	82.9105	0.01%	455.92	455.9501	0.01%
	40	20	7.27	7.268	-0.03%	15.14	15.1386	-0.01%
		200	27.38	27.3833	0.01%	96.76	96.7614	0.00%
		2000	112.02	112.0062	-0.01%	717.50	717.5328	0.00%
50	0	20	4.95	4.9517	0.03%	7.83	7.8295	-0.01%
		200	12.88	12.8803	0.00%	27.05	27.0522	0.01%
		2000	34.48	34.4809	0.00%	98.50	98.5026	0.00%
	10	20	5.73	5.7321	0.04%	9.70	9.697	-0.03%
		200	17.22	17.2159	-0.02%	41.93	41.9261	-0.01%
		2000	54.10	54.1031	0.01%	198.51	198.5201	0.01%
	20	20	6.55	6.547	-0.05%	11.88	11.8814	0.01%
		200	22.40	22.3978	-0.01%	62.65	62.6499	0.00%
		2000	81.64	81.6564	0.02%	374.23	374.2545	0.01%
	30	20	7.36	7.3591	-0.01%	14.29	14.2908	0.01%
		200	28.19	28.1934	0.01%	88.50	88.505	0.01%
		2000	117.19	117.2000	0.01%	631.69	631.7188	0.00%
	40	20	8.13	8.1286	-0.02%	16.78	16.7787	-0.01%
		200	34.22	34.2260	0.02%	117.19	117.1981	0.01%
		2000	158.71	158.8893	0.11%	942.33	942.4156	0.01%
	50	20	8.82	8.8168	-0.04%	19.16	19.1646	0.02%
		200	40.03	40.0312	0.00%	145.63	145.6395	0.01%
		2000	202.97	202.8884	-0.04%	1259.29	1259.3472	0.00%

Table 3 The results (r_b/a) of the presented solution for different k_0=1 and k=1

φ0	ψ0	k0=0.2	k0=0.4	k0=0.6	k0=0.8	k0=1.0	Difference (%)
20	0	10.3538	7.3766	6.0598	5.2758	4.7411	118.38%
	10	15.0659	10.1424	8.0655	6.8641	6.0621	148.53%
	20	21.4629	13.6895	10.5553	8.7919	7.6379	181.01%
30	0	8.6249	6.1615	5.0712	4.4216	3.9783	116.80%
	10	12.0217	8.1337	6.4905	5.5386	4.9022	145.23%
	20	16.366	10.5233	8.1586	6.8243	5.9489	175.11%
	30	21.5889	13.2582	10.0161	8.2292	7.0766	205.07%
40	0	7.6576	5.4816	4.5176	3.9427	3.5502	115.69%
	10	10.3648	7.042	5.6347	4.8181	4.2713	142.66%
	20	13.6779	8.8569	6.8978	5.789	5.0597	170.33%
	30	17.4835	10.85	8.2511	6.8119	5.8801	197.33%
	40	21.5577	12.9041	9.6169	7.83	6.6881	222.33%
50	0	7.0548	5.0574	4.1717	3.6432	3.2819	114.96%
	10	9.3531	6.3755	5.1119	4.3774	3.8851	140.74%
	20	12.0753	7.8638	6.1459	5.171	4.5284	166.66%
	30	15.0992	9.4505	7.224	5.986	5.1818	191.39%
	40	18.2329	11.0403	8.2846	6.7781	5.8112	213.75%
	50	21.2419	12.5269	9.2624	7.5014	6.3819	232.85%

Table 4 The results (r_b/a) of the presented solution for different k_0 and k=2

φ0	ψ0	k0=0.2	k0=0.4	k0=0.6	k0=0.8	k0=1.0	Difference (%)
20	0	4.3858	3.5107	3.0873	2.8208	2.6316	66.66%
	10	6.0395	4.5961	3.9274	3.5176	3.2321	86.86%
	20	8.3803	6.0529	5.022	4.4071	3.9872	110.18%
30	0	3.8286	3.0743	2.709	2.4788	2.3153	65.36%
	10	5.0177	3.8466	3.3024	2.9679	2.7344	83.50%
	20	6.5467	4.7964	4.0146	3.5455	3.2237	103.08%
	30	8.3898	5.8984	4.8243	4.1934	3.7669	122.72%
40	0	3.491	2.8093	2.4786	2.27	2.1215	64.55%
	10	4.4195	3.4084	2.9366	2.6457	2.4422	80.96%
	20	5.5285	4.0992	3.4549	3.066	2.7977	97.61%
	30	6.7588	4.8462	4.0082	3.5108	3.1719	113.08%
	40	8.0155	5.5982	4.561	3.9532	3.5428	126.25%
50	0	3.2665	2.6322	2.324	2.1293	1.9904	64.11%
	10	4.0339	3.1253	2.6996	2.4363	2.2516	79.16%
	20	4.9018	3.6681	3.1074	2.7671	2.5313	93.65%
	30	5.8104	4.2276	3.5248	3.1041	2.8156	106.36%
	40	6.6893	4.7663	3.9259	3.4277	3.0884	116.59%
	50	7.4759	5.2496	4.2863	3.7189	3.3344	124.21%

Table 5 The results (p/σ_{h0}) of the presented solution for different k_0 and k=1

φ0	ψ0	k0=0.2	k0=0.4	k0=0.6	k0=0.8	k0=1.0	Difference (%)
20	0	4.4171	3.7161	3.3618	3.1325	2.9665	48.90%
	10	5.3477	4.3709	3.8892	3.5822	3.3624	59.04%
	20	6.4048	5.0928	4.4608	4.0639	3.7827	69.32%
30	0	6.3083	5.0412	4.4274	4.0408	3.766	67.51%
	10	7.8714	6.0664	5.2191	4.6955	4.3285	81.85%
	20	9.6686	7.2029	6.0788	5.3965	4.9246	96.33%
	30	11.6294	8.4022	6.9695	6.1138	5.5287	110.35%
40	0	8.0802	6.2202	5.3466	4.8064	4.4276	82.50%
	10	10.24	7.5673	6.3558	5.6229	5.117	100.12%
	20	12.7223	9.0547	7.4458	6.4916	5.8424	117.76%
	30	15.4168	10.6133	8.5662	7.3731	6.5714	134.60%
	40	18.1629	12.1555	9.6572	8.2222	7.268	149.90%
50	0	9.6178	7.2056	6.0973	5.4211	4.9517	94.23%
	10	12.2834	8.8091	7.2728	6.3573	5.7321	114.29%
	20	15.3308	10.5677	8.5332	7.3458	6.547	134.17%
	30	18.6107	12.3944	9.8176	8.3403	7.3591	152.89%
	40	21.9187	14.1841	11.0565	9.2897	8.1286	169.65%
	50	25.0244	15.827	12.1801	10.1438	8.8168	183.83%

Table 6 The results (p/σ_{h0}) of the presented solution for different k_0 and k=2

φ0	ψ0	k0=0.2	k0=0.4	k0=0.6	k0=0.8	k0=1.0	Difference (%)
20	0	6.8362	5.4486	4.7796	4.3593	4.0614	68.32%
	10	9.4724	7.1705	6.1086	5.4595	5.0082	89.14%
	20	13.2274	9.4938	7.8484	6.8701	6.2034	113.23%

Table 6 Continued

φ0	ψ0	k0=0.2	k0=0.4	k0=0.6	k0=0.8	k0=1.0	Difference (%)
30	0	10.7805	8.0459	6.7972	6.0384	5.513	95.55%
	10	15.4616	10.8482	8.8515	7.6769	6.8824	124.65%
	20	22.0431	14.559	11.4843	9.7311	8.5714	157.17%
	30	30.6841	19.1818	14.6721	12.1713	10.5495	190.86%
40	0	14.7935	10.5292	8.6551	7.5423	6.7845	118.05%
	10	21.3975	14.2493	11.2854	9.5857	8.4567	153.02%
	20	30.3777	19.0209	14.5548	12.0733	10.4615	190.38%
	30	41.603	24.7181	18.3638	14.9246	12.7324	226.75%
	40	54.329	30.979	22.4795	17.971	15.1386	258.88%
50	0	18.4929	12.7151	10.2443	8.801	7.8295	136.20%
	10	26.6687	17.128	13.2849	11.1186	9.697	175.02%
	20	37.3971	22.6134	16.958	13.8664	11.8814	214.75%
	30	50.231	28.9295	21.1026	16.9263	14.2908	251.49%
	40	64.1379	35.6218	25.4414	20.104	16.7787	282.26%
	50	77.7824	42.1203	29.6299	23.1599	19.1646	305.86%

the five different values of k_0, i.e., 0.2, 0.4, 0.6, 0.8, and 1.0 are considered, and the other calculation parameters are selected by based on Yu (2002) and Tables 3 and 4. Table 3 show the evolution of the r_b/a against φ and ψ. The ratio of the r_b/a is 10.3538 when k_0=0.2, $\varphi=20^0$and $\psi=0^0$, which becomes 4.7411 when k_0=1.0, $\varphi=20^0$ and $\psi=0^0$. Comparing with k_0=1.0, the value of the r_b/a with k_0=0.2 decreases by 118.38% as shown in Table 3. In Table 4, the r_b/a also shows the same tendency with k_0 varying from 0.2 to 1.0. Comparing with k_0=1.0, the value of the r_b/a with k_0=0.2 decreases by 66.66% as shown in Table 4. Therefore, the results show that the ratio decreases with the increase in $0.2<k_0<1.0$. This observation suggests that it also is indicate that ignoring the effect of initial anisotropic stress factor k_0 on the r_b/a will be miscalculated results, and an appropriate estimation of the k_0 value is essential for the cavity pressure because it is usually calculated from σ_v in engineering practice. As shown in tables 3 and 4, with the factor k_0 varying from 0.2 to 1.0, the r_b/a decreases with the increase of initial anisotropic stress factor k_0 for k=1 and k=2.

The kind of displacement solution of the created cavity expansion problem based on Cam-Clay model is produced for cylindrical cavities which model the action of the pressuremeter, and for spherical cavities that may be used to estimate cone tip resistance and bearing capacity of displacement piles (Collins and Yu 1996), as well as that may be used to estimate lateral displacement of displacement piles (Chai *et al.* 2005). This observation suggests that the presented solution is a useful tool for the design of soft subsoil improvement resulting from the pile installation.

It is interesting to note here that, to investigate the effect of the initial value of k_0 on the normalized internal pressure (p/σ_{h0}) of cavity expansion problem, five cases with the same other parameters but different values of k_0 are also studied, the five different values of k_0, i.e., 0.2, 0.4, 0.6, 0.8, and 1.0 are considered, and the other calculation parameters are selected by based on Yu (2002) and Tables 5 and 6. Table 5 show the evolution of the ratio of the cavity pressure to σ_{h0} against φ and ψ. The ratio of the limiting pressure to the initial pressure (σ_{h0}) is 4.4171 when k_0= 0.2, $\varphi=20^0$ and $\psi=0^0$, which becomes 2.9665 when k_0= 1.0, $\varphi=20^0$ and $\psi=0^0$. Comparing with k_0=1.0, the value of the ratio of the cavity pressure to σ_{h0} with k_0=0.2 decreases by 48.90% as shown in Table 5. In Table 6, the ratio of the cavity pressure to σ_{h0} also shows the same tendency with k_0 varying from 0.2 to 1.0. Comparing with k_0=1.0, the value of the ratio of the cavity pressure to σ_{h0} with k_0=0.2 decreases by 68.32% as shown in Table 6. Therefore, the results show that the ratio decreases with the increase in $0.2<k_0<1.0$. This observation suggests that it also is indicate that ignoring the effect of initial anisotropic stress factor k_0 on the p/σ_{h0} will also be miscalculated results, as well as the same tendency of the ratio of the cavity pressure to σ_{h0} with k_0 varying from 0.4 to 1.0 in paper of Su and Yang (2019). As shown in tables 5 and 6, With the factor k_0 varying from 0.2 to 1.0, the p/σ_{h0} decreases with the increase of initial anisotropic stress factor k_0 for k=1 and k=2.

In addition, with the internal friction angle (φ) varying from 20^0 to 50^0 degrees, the r_b/a increases with the increase of the φ for k=1 and k=2, and the p/σ_{h0} increases with the increase of the φ for k=1 and k=2. Similarly, With the dilation angle (ψ) varying from 0^0 to φ degrees, the r_b/a increases with the increase of the dilation angle (ψ) for k=1 and k=2, and the p/σ_{h0} increases with the increase of the ψ for k=1 and k=2. Finally, The relative difference of k_0=0.2 and k_0=1.0 increases with the increase of the φ and the ψ for k=1 and k=2. The solution in this study also provides a new idea and method for solving the cavity expansion problem by using critical state model. It can be applied to the study of geotechnical problems such as static penetration test and jacked piles in dilatant soils. It has certain theoretical significance for perfecting and enriching the theory of elasto-plastic cavity expansion (Li *et al.*, 2017).

4. Conclusions

On the basis of the Cam-Clay model and considering the effect of initial anisotropic stress and drained conditions, a novel theoretical solution for created cavity expansion problem are investigated in this study for the first time. Compared with the previous solutions, the following improvements have been achieved:

(1) The proposed solution eliminates the limitation of the condition of initial isotropic stress which is usually required by existing results, so it can be applied to more general cases.

(2) A general drained solution is proposed in this study, which is rather different from the existing results that are usually based on the isotropic and undrained conditions.

(3) The parametric study is presented in order to the engineering significance of this work, the initial stress state of natural soil mass is anisotropy by soil deposition and consolidation. With the factor k_0 varying from 0.2 to 1.0, the r_b/a decreases with the increase of initial anisotropic stress factor k_0 for k=1 and k=2, and the p/σ_{h0} decreases with the increase of initial anisotropic stress factor k_0 for k=1 and k=2, it is indicate that ignoring the effect of initial anisotropic stress factor k_0 on the r_b/a and the p/σ_{h0} will be miscalculated results.

Acknowledgments

This work was supported by the National Key R&D Program of China (2017YFB1201204). The first author thanks Project 2018zzts188 supported by Innovation Foundation for Postgraduate of the Central South University. The editor's and anonymous reviewer's comments have improved the quality of the study and are also greatly acknowledged.

References

Andersen, K.H. (1980), "Cyclic and static laboratory tests on Drammen clay", *J. Geotech. Eng. Div.*, **106**(5), 499-529.

Bishop, R.F., Hill, R. and Mott, N.F. (1945), "Theory of identation and hardness tests", *Proc. Phys. Soc.*, **57**, 147-159.

Cao, L.F., Teh, C.I. and Chang, M.F. (2001), "Undrained cavity expansion in modified cam clay I: Theoretical analysis", *Géotechnique*, **51**(4), 323-334. https://doi.org/10.1680/geot.2001.51.4.323.

Chai, J.C., Miura, N. and Koga, H. (2005), "Lateral displacement of ground caused by soil–cement column installation", *J. Geotech. Geoenviron. Eng.*, **131**(5), 623-632. https://doi.org/10.1061/(ASCE)1090-0241(2005)131:5(623).

Chen, G.H., Zou, J.F. and Qian, Z.H. (2019), "An improved collapse analysis mechanism for the face stability of shield tunnel in layered soils", *Geomech. Eng.*, **17**(1), 97-107. https://doi.org/10.12989/gae.2019.17.1.097.

Chen, S.L. and Abousleiman, Y.N. (2012), "Exact undrained elasto-plastic solution for cylindrical cavity expansion in modified cam clay soil mass", *Géotechnique*, **62**(5), 447-456. https://doi.org/10.1680/geot.11.P.027.

Chen, S.L. and Abousleiman, Y.N. (2017), "Cavity expansion in strain hardening frictional soils under drained condition", *Int. J. Numer. Anal. Meth. Geomech.*, **42**(1), 132-142. https://doi.org/10.1002/nag.2718.

Collins, I.F. and Yu, H.S. (1996), "Undrained cavity expansions in critical state soils", *Int. J. Numer. Anal. Meth. Geomech.*, **20**(7), 489-516. https://doi.org/10.1002/(SICI)1096-9853(199607)20:7<489::AID-NAG829>3.0.CO;2-V.

Diao, H, Wu, Y., Liu, J. and Luo, R. (2015), "An analytical investigation of soil disturbance due to sampling penetration", *Geomech. Eng.*, **9**(6), 743-755. http://dx.doi.org/10.12989/gae.2015.9.6.743.

Frikha, W. and Bouassida, M. (2014), "Prediction of stone column ultimate bearing capacity using expansion cavity model", *Proc. Inst. Civ. Eng. Ground Improv.*, **168**(2), 106-115. https://doi.org/10.1680/grim.13.00045.

Frikha, W., Bouassida, M. and Stuedlein, A.W. (2015), "Discussion: Prediction of stone column ultimate capacity using cavity expansion model", *Proc. Inst. Civ. Eng. Ground Improv.*, **168**(3), 231-234.

Hill, R. (1950), *The Mathematical Theory of Plasticity*, Clarendon Press.

Hill, R., Mott, N.F. and Pack, D.C. (1944), "Penetration of Munroe jets", Armament Research Department Report 2/44, U.K.

Keawsawasvong, S. and Ukritchon, B. (2016), "Ultimate lateral capacity of two-dimensional plane strain rectangular pile in clay", *Geomech. Eng.*, **11**(2), 235-252. http://dx.doi.org/10.12989/gae.2016.11.2.235.

Kwon, J., Kim, C., Im, J.C. and Yoo, J.W. (2018), "Effect of performance method of sand compaction piles on the mechanical behavior of reinforced soft clay", *Geomech. Eng.*, **14**(2), 175-185. https://doi.org/10.12989/gae.2018.14.2.175.

Li, C. and Zou, J.F. (2019a), "Closed-form solution for undrained cavity expansion in anisotropic soil mass based on the spatially mobilized plane failure criterion", *Int. J. Geomech.*, **19**(7), 04019075. https://doi.org/10.1061/(ASCE)GM.1943-5622.0001458.

Li, C., Zou, J.F. and Zhou, H. (2019b), "Cavity expansions in k0 consolidated clay", *Eur. J. Environ. Civ. Eng.*, https://doi.org/10.1080/19648189.2019.1605937.

Li, G.X. (2004), *Higher Soil Mechanics*, Tsinghua University Press (in Chinese).

Li, L., Li, J. and Sun, D. (2016), "Anisotropically elasto-plastic solution to undrained cylindrical cavity expansion in K0-consolidated clay", *Comput. Geotech.*, **73**, 83-90. https://doi.org/10.1016/j.compgeo.2015.11.022.

Li, L., Li, J.P., Sun, D.A. and Li, X F. (2017), "Elasto-plastic solution to expansion of a spherical cavity in dilatant sand", *Chin. J. Geotech. Eng.*, **39**(8), 1454-1460 (in Chinese).

Lukic, D.C., Prokic, A.D. and Brcic, S.V. (2014), "Stress state around cylindrical cavities in transversally isotropic rock mass", *Geomech. Eng.*, **6**(3), 213-233. https://doi.org/10.12989/gae.2014.6.3.213.

Marchi, M., Gottardi, G. and Soga, K. (2014), "Fracturing pressure in clay", *J. Geotech. Geoenviron. Eng.*, **140**(2), 04013008. https://doi.org/10.1061/(ASCE)GT.1943-5606.0001019.

Park, K.H., Tontavanich, B. and Lee, J.G. (2008), "A simple procedure for ground response curve of circular tunnel in elastic-strain softening rock masses", *Tunn. Undergr. Sp. Technol.*, **23**(2), 151-159. https://doi.org/10.1016/j.tust.2007.03.002.

Pournaghiazar, M., Russell, A.R. and Khalili, N. (2013), "Drained cavity expansions in soils of finite radial extent subjected to two boundary conditions", *Int. J. Numer. Anal. Meth. Geomech.*, **37**(4), 331-352. https://doi.org/10.1002/nag.1099.

Randolph, M.F. (2003), "Science and empiricism in pile foundation design", *Géotechnique*, **53**(10), 847-876. https://doi.org/10.1680/geot.2003.53.10.847.

Roscoe, K.H., Schofield, A. and Wroth, A.P. (1958), "On the yielding of soils", *Geotechnique*, **8**(1), 22-53. https://doi.org/10.1680/geot.1958.8.1.22.

Roscoe, K.H., Schofield, A.N. and Thurairajah, A. (1963), "Yielding of clay in states wetter than critical", *Geotechnique,* **13**(3), 211-240. https://doi.org/10.1680/geot.1963.13.3.211.

Russell, A.R. and Khalili, N. (2002), "Drained cavity expansion in sands exhibiting particle crushing", *Int. J. Numer. Anal. Meth. Geomech.*, **26**(4), 323-340. https://doi.org/10.1002/nag.203.

Salgado, R. and Randolph, M.F. (2001), "Analysis of cavity expansion in sand", *Int. J. Geomech.*, **1**(2), 175-192. https://doi.org/10.1061/(ASCE)1532-3641(2001)1:2(175).

Schofield, A.N. and Wroth, C.P. (1968), *Critical State Soil Mechanics*, McGraw-Hill, London, U.K.

Seo, H.J., Jeong, K.H., Choi, H. and Lee, I.M. (2012), "Pullout resistance increase of soil nailing induced by pressurized grouting", *J. Geotech. Geoenviron. Eng.*, **138**(5), 604-613. https://doi.org/10.1061/(ASCE)GT.1943-5606.0000622.

Sivasithamparam, N. and Castro, J. (2018), "Undrained expansion of a cylindrical cavity in clays with fabric anisotropy: Theoretical solution", *Acta Geotech.*, **13**(3), 729-746. https://doi.org/10.1007/s11440-017-0587-4.

Su, D. and Yang, Z.X. (2019), "Drained analyses of cylindrical cavity expansion in sand incorporating a bounding-surface model with state-dependent dilatancy", *Appl. Math. Model.*, **68**, 1-20. https://doi.org/10.1016/j.apm.2018.11.017.

Teh, C.I. and Houlsby, G.T. (1991), "Analytical study of the cone penetration test in clay", *Geotechnique*, **41**(1), 17-34. https://doi.org/10.1680/geot.1991.41.1.17.

Tolooiyan, A. and Gavin, K. (2011), "Modelling the cone penetration test in sand using cavity expansion and arbitrary Lagrangian Eulerian finite element methods", *Comput. Geotech.,* **38**(4), 482-490. https://doi.org/10.1016/j.compgeo.2011.02.012.

Vesic, A.S. (1972), "Expansion of cavities in infinite soil mass", *J. Soil Mech. Found. Div.*, **98**(3), 265-290.

Vesic, A.S. (1977), "Design of pile foundations", NCHRP Synthesis of Highway Practice, Vol. 42., Transportation Research Board, Washington, D.C., U.S.A.

Wang, S., Yin, S. and Wu, Z. (2012a), "Strain-softening analysis of a spherical cavity", *Int. J. Numer. Anal. Meth. Geomech.*, **36**(2), 182-202. https://doi.org/10.1002/nag.1002.

Wang, S., Yin, X., Tang, H. and Ge, X. (2012b), "A new approach for analyzing circular tunnel in strain-softening rock masses", *Int. J. Rock Mech. Min. Sci.*, **47**(1), 170-178.

Xiao, Y. and Desai, C.S. (2016), "General stress-dilatancy relation for granular soils", *J. Geotech. Geoenviron. Eng.*, **142**(4), 02816001. https://doi.org/10.1061/(ASCE)GT.1943-5606.0001473.

Yu, H.S. and Carter, J.P. (2002), "Rigorous similarity solutions for cavity expansion in cohesive-frictional soils", *Int. J. Geomech.*, **2**(2), 233-258. https://doi.org/10.1061/(ASCE)1532-3641(2002)2:2(233).

Yu, M.H. (2004), *Unified Strength Theory and Applications*, Springer-Verlag Berlin Heidelberg, New York, U.S.A.

Zhou, H., Kong, G., Liu, H. and Laloui, L. (2018), "Similarity solution for cavity expansion in thermoplastic soil", *Int. J. Numer. Anal. Meth. Geomech.*, **42**(2), 274-294. https://doi.org/10.1002/nag.2724.

Zhou, H., Liu, H., Kong, G. and Huang, X. (2014), "Analytical solution of undrained cylindrical cavity expansion in saturated soil under anisotropic initial stress", *Comput. Geotech.*, **55**, 232-239. https://doi.org/10.1016/j.compgeo.2013.09.011.

Zou, J.F., Chen, G. and Qian, Z. (2019a), "Tunnel face stability in cohesion-frictional soils considering the soil arching effect by improved failure models", *Comput. Geotech.*, **106**, 1-17. https://doi.org/10.1016/j.compgeo.2018.10.014.

Zou, J.F., Chen, K.F. and Pan, Q.J. (2017), "Influences of seepage force and out-of-plane stress on cavity contracting and tunnel opening", *Geomech. Eng.*, **13**(6), 907-928. https://doi.org/10.12989/gae.2017.13.6.907.

Zou, J.F., Yang, T., Wang, L., Guo, W.J. and Huang, F.L. (2019b), "A numerical stepwise approach for cavity expansion problem in strain-softening rock or soil mass", *Geomech. Eng.*, **18**(3), 225-234. https://doi.org/10.12989/gae.2019.18.3.225.

CC